

ULTIMATE VERTICAL BEARING CAPACITY OF CLAYEY SQUEEZE BREAKDOWN USING RIGID-PLASTIC FINITE ELEMENT METHOD

*Kazuhiro KANEDA¹, Masamichi AOKI¹, Tomohiro TANIKAWA¹ and Satoru OHTSUKA²

¹Reseachr, Takenaka Corporation, Japan; ²Department of Civil and Environmental Engineering Nagaoka University of Technology, Japan

*Corresponding Author, Received: 19 Dec. 2018, Revised: 04 Feb. 2019, Accepted: 23 Feb. 2019

ABSTRACT: The relations of ultimate bearing capacity for foundations are specified in the guideline published by the Architectural Institute of Japan for design of building foundations. The rigid-plastic finite element method developed by Tamura and Ohtsuka has been employed to estimate the ultimate bearing capacity of footings. The characteristic of this method is that, in contrast to deformation analysis, it applies limited soil constants; only the strength parameters, such as cohesion and friction angle, are used since the method deals with the limit state directly by disregarding the deformation of the building and ground. In this study, a series of rigid plastic finite element analyses were performed to compare the ultimate bearing capacities of spread foundation for clayey squeeze breakdown obtained by simulations and the formulae of the Architectural Institute of Japan. The change in the failure mode of the ground was discussed considering the geometrical ratio between the width of the footing and the surface clay layer. In addition, inclined load was considered for clayey squeeze breakdown. The applicability of rigid plastic FEM to the assessment of ultimate vertical bearing capacity of clayey squeeze breakdown was demonstrated.

Keywords: Clayey squeeze breakdown, Ultimate bearing capacity, Rigid plastic FEM, Inclined load

1. INTRODUCTION

The calculation of the ultimate bearing capacity of soil (Terzaghi et al., 1967) is important when designing a building. The ultimate bearing capacity formulae for building foundations are specified in the guideline published by the Architectural Institute of Japan (AIJ).(AIJ, 2001) These formulae were proposed based on experiments and theoretical considerations avoiding some risk. However, the inclined bearing capacity was not adequately investigated yet. In this research, the vertical bearing capacity of spread foundation with a thin clay layer was analyzed using numerical simulations. First, the clayey squeeze breakdown was simulated (Kaneda et al., 2013), and subsequently, the associated inclined bearing capacity was discussed. The analysis uses the rigid-plastic finite element method. The rigid-plastic finite element method (RPFEM), developed by Tamura and Ohtsuka (T. Tamura et al., 1984 and A. Asaoka and S. Ohtsuka, 1986), was employed to estimate the ultimate bearing capacity of footing. The Drucker-Prager yield function was adopted as the soil constitutive equation and the associate and non-associate flow rules were introduced to establish the configuration relationship of the ultimate state. Using this method, the structural safety assessment or calculation of soil bearing capacity was evaluated.

The characteristic of this method is that, in contrast with deformation analysis, it applies limited soil constants; it only uses the strength parameters, such as cohesion and friction angle, because it deals with the limit state directly by disregarding the deformation of the building and ground. Since RPFEM uses the upper bound theorem of plastic theory, it becomes slightly larger than the true value. In this paper, at first, a brief formulation of RPFEM was shown. Then, the squeeze breakdown was discussed and the results of numerical analysis and discussions were described.

2. THE CONSTITUTIVE EQUATION FOR RIGID PLASTIC FINITE ELEMENT METHOD

Tamura (Tamura et al., 1984) developed the rigid plastic constitutive equation for frictional material. The Drucker-Prager's type yield function is expressed as follows.

$$f(\sigma) = \alpha I_1 + \sqrt{J_2} - k = 0 \quad (1)$$

where, I_1 is the first invariant of stress σ_{ij} and $I_1 = tr(\sigma_{ij})$ in which extension stress is defined positive.

J_2 is the second invariant of deviator stress S_{ij} and $J_2 = \frac{1}{2} S_{ij} S_{ij}$ and the coefficients,

$\alpha = \frac{\tan\phi}{\sqrt{9+12\tan^2\phi}}$ and $k = \frac{3c}{\sqrt{9+12\tan^2\phi}}$ and the material constants corresponding to shear resistance angle and cohesion under the plane strain condition. The volumetric strain rate is expressed as follows:

$$\varepsilon_v = \text{tr}(\dot{\boldsymbol{\varepsilon}}) = \text{tr}\left(\lambda \frac{\partial f(\boldsymbol{\sigma})}{\partial \boldsymbol{\sigma}}\right) = \text{tr}\left(\lambda \left(\alpha \mathbf{I} + \frac{s}{2\sqrt{J_2}}\right)\right) = \frac{3\alpha}{\sqrt{3\alpha^2 + \frac{1}{2}}}\dot{\varepsilon} \quad (2)$$

where, λ is an indeterminate multiplier and \mathbf{I} is the unit tensor. The strain rate $\dot{\boldsymbol{\varepsilon}}$ which is purely plastic component should satisfy the volumetric constraint condition as follow:

$$h(\dot{\boldsymbol{\varepsilon}}) = \dot{\varepsilon}_v - \frac{3\alpha}{\sqrt{3\alpha^2 + \frac{1}{2}}}\dot{\varepsilon} = \dot{\varepsilon}_v - \eta\dot{\varepsilon} = 0 \quad (3)$$

in which $\dot{\varepsilon}_v$ and $\dot{\varepsilon}$ indicate the volumetric strain rate and the norm of strain rate, respectively. The parameter η is defined in Eq. (3). The rigid plastic constitutive equation is expressed by Lagrangian method after Tamura (1991) as follows:

$$\boldsymbol{\sigma} = \frac{k}{\sqrt{3\alpha^2 + \frac{1}{2}}}\frac{\dot{\boldsymbol{\varepsilon}}}{\dot{\varepsilon}} + \beta \left(\mathbf{I} - \eta \frac{\dot{\boldsymbol{\varepsilon}}}{\dot{\varepsilon}}\right) \quad (4)$$

where, β represents a Lagrangian multiplier which indicates the equilibrating stress satisfying the yield function expressed by Eq.(1). Moreover, the constraint condition on strain rate is introduced into the constitutive equation directly with the use of penalty method (Hoshina et al., 2011; Nguyen Du L. et al., 2016). The stress-strain rate relation for the Drucker-Prager's yield function is expressed as follow:

$$\boldsymbol{\sigma} = \frac{k}{\sqrt{3\alpha^2 + \frac{1}{2}}}\frac{\dot{\boldsymbol{\varepsilon}}}{\dot{\varepsilon}} + \kappa(\dot{\varepsilon}_v - \eta\dot{\varepsilon}) \left(\mathbf{I} - \eta \frac{\dot{\boldsymbol{\varepsilon}}}{\dot{\varepsilon}}\right) \quad (5)$$

where κ is a penalty constant. FEM with this constitutive equation provides the equivalent equation of the upper bound theorem in plasticity so that this method is called as RPFEM in this study. It is noted property of this constitutive equation that the relationship between stress and strain rate is specified. The norm of strain rate is substantially indeterminate since the limit state of structure is focused. Stress is determined for normalized strain rate using its norm. In order to determine the limit load coefficient for the prescribed load Hoshina et al. (2011) introduced the constraint condition on external work into the equilibrium equation by using the penalty method. It reported the rational result was obtained by the developed method in comparison with the previous

works. The use of penalty method was profited computation time efficiency and obtaining stable computational result.

3. SIMULATIONS OF CLAYER SQUEEZE BREAKDOWN WITHOUT INITIAL LOAD

3.1 What is the clayey squeeze breakdown?

Consider a soft clay upper rigid foundation of height H , as shown in figure 1 (H. Yamaguchi, 1990). When the foundation width B becomes larger than the layer height H , the failure mode shifts from the general failure mode, specified by Terzaghi (Terzaghi et al., 1967), to that of the squeeze breakdown, wherein the upper clay layer is pushed out to both sides in plastic state. The bearing capacity of squeeze breakdown can be expressed as the following equation (Meyerhof et al., 1953).

$$q_f = 4.14c_u + \frac{c_u B}{2H} \quad (6)$$

where q_f , c_u , B , and H are the ultimate bearing capacity of squeeze breakdown (kN/m²), undrained strength (kN/m²), foundation width (m), and clay layer height (m), respectively.

When the relationship between B and H is

$$B/H \geq \sqrt{2} \quad (7)$$

squeeze breakdown occurs.

In addition, with regard to the general failure mode, AIJ proposed the following equation for ultimate bearing capacity.

$$q_u = (i_c \cdot \alpha \cdot c_u \cdot N_c + i_\gamma \cdot \beta \cdot \gamma_1 \cdot B \cdot \eta \cdot N_\gamma + i_q \cdot \gamma_2 \cdot D_f \cdot N_q) \quad (8)$$

where q_u is the ultimate vertical bearing capacity (kN/m²), N_c , N_γ , N_q are the coefficients of bearing capacity, γ_1 is the unit weight of soils (kN/m³), and γ_2 is the unit weight of the penetration area (kN/m³). α , β are the shape coefficients, η is the correction factor for the foundation size, i_x , i_γ , i_q are the correction factors of inclined load, and D_f is the penetration length (m).

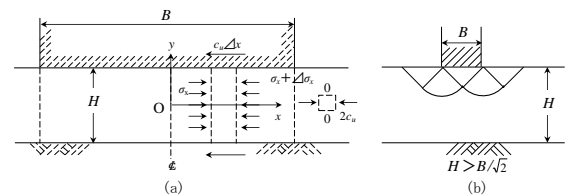


Fig. 1 Outline of squeeze breakdown.

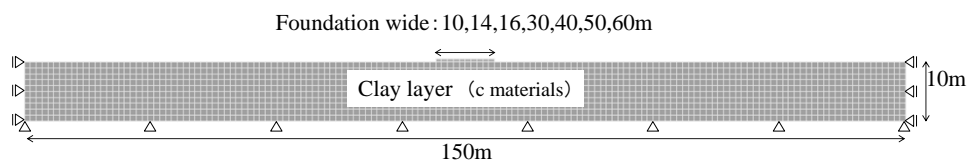


Fig. 2 Analysis mesh.

3.2 Numerical conditions

Figure 2 shows the numerical mesh, which is 150 m wide and 10 m high in the plane strain condition. The foundation widths were set as 10, 14, 16, 30, 40, and 50 m. Assuming a rigid foundation, the strength of foundation was set as $c_u = 1000000 \text{ kN/m}^2$. The soil layer was assumed to be homogeneous type c material. The inclined load (horizontal load/vertical load (F/V)) was set as 0.1, 0.2, 0.3, 0.4, and 0.5.

3.3 Numerical results

3.3.1 Vertical bearing capacity

Table 1 shows the results of the simulation using equation (6). Using equation (7), squeeze breakdown was applied to the over 14 m-wide foundation ($B/H=1.4$). Figure 3 shows the relationship between N_c and B/H . N_c is the value divided three numerical results by $c_u = 10 \text{ kN/m}^2$. From the simulation results, it can be observed that when the foundation width ratio (B/H) is large, N_c is also large for the squeeze breakdown. Figure 4 shows the pattern of the failure mode according the foundation width ratio as per Yamaguchi (Yamaguchi, 1982). The tearing failure was accompanied by tensile cracks. It is important to clarify the mechanism of tearing; however, it is difficult to evaluate the extension strength using the Drucker–Prager yield function and would thus be future work. In this simulation, it is necessary to consider the extension strength. Without it, the squeeze breakdown was simulated well using the rigid-plastic FEM. Figure 5 shows the contours of the shear strain at the point of failure. The general failure mode occurred at the foundation width of 10 m ($B/H=1.0$), the failure surface touched the bottom for the foundation width of 16 m ($B/H=1.6$), the cross-shaped shear surface occurred at 30 m foundation width ($B/H=3.0$). For the 40 m-foundation width ($B/H=4.0$), the cross-shaped shear surface cannot be seen; squeeze breakdown occurred at both sides of the lower end of the foundation. The calculation of the bearing capacity of squeeze breakdown was performed by assuming that the clay under the foundation was pushed to both sides due to the application of the upper load. Somewhat complicated destruction forms can be seen in figures 5(e) and (f) that show the occurrence of the fan shape failure mode and rigid passive mode at 45° . Although the simulation could not correctly provide the failure mode shown in figure 4, the other bearing capacity values and failure modes obtained with this theory were mostly correct.

Table 1 Comparison of numerical results and theoretical values

	B/H	Bearing theoretical value kN/m ²	Bearing numerical analysis value kN/m ²	Numerical analysis value / Theoretical value	N_c (Numerical analysis value)
General failure mode	-	51.40			
Clayey squeeze breakdown	1.00	46.40	52.71	0.88	5.27
	1.40	48.40	52.53	0.92	5.25
	1.60	49.40	52.93	0.93	5.29
	3.00	56.40	58.78	0.96	5.88
	4.00	61.40	63.91	0.96	6.39
	5.00	66.40	69.23	0.96	6.92
	6.00	71.40	74.47	0.96	7.45

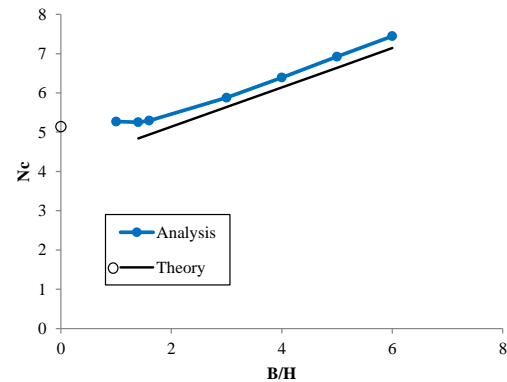


Fig. 3 Relationship between N_c and B/H .

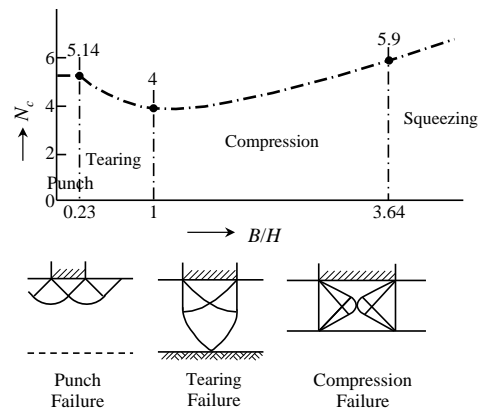
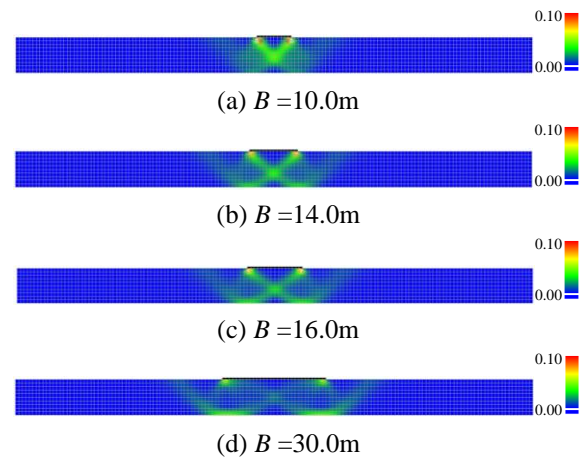


Fig. 4 Pattern of failure mode according to the foundation width ratio.



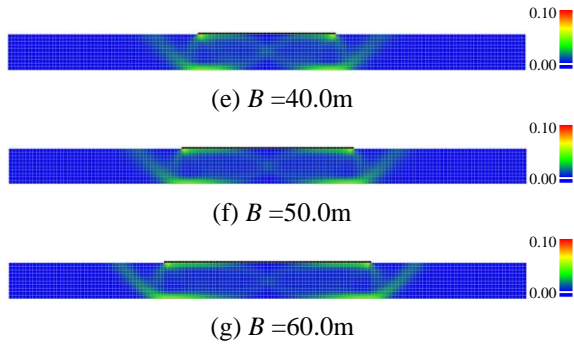


Fig. 5 Contours of shear strain at the failure.

3.3.1 Inclined bearing capacity

Simulations were performed for both the vertical and horizontal load. Figure 6 shows the numerical results of the relationship between N_c and F/V using AIJ equations (8) and (9); the legend shows the B/H .

In AIJ, inclined load is considered by the following formula.

$$i_c = (1 - \theta/90)^2 \quad (9)$$

where θ is the inclination angle ($^\circ$).

In the case of $F/V=0$, N_c increases as B/H increases. However, in the case of $F/V=0.2$, the value of each B/H are almost the same. In the case of a larger F/V , a large value of B/H corresponds to a small supporting force. In the AIJ equation (8), the general failure mode was adopted considering the inclined load; however, the inclined load of the squeeze breakdown was not described.

For $F/V > 0.2$, the numerical results are nearly equal to those obtained by equation (9). It is therefore indicated that the general failure mode occurred instead of squeeze breakdown. Figures 7 and 8 show the contours of shear strain at the failure point for each foundation width. At large F/V , a large value of B/H is not obtained at the squeeze breakdown because the failure area becomes shallow. However, when both B/H and F/V are large, the failure slip is restricted to the bottom. Therefore, it was considered that the opposite condition occurred, which entails that the bearing capacity associated with a large B/H is smaller than that with small B/H . In earthquake architectural design, the value F/V is almost over 0.2. When detailed bearing capacity analysis is not performed for the case of a large B/H , it is considered better to use the bearing capacity value of the general failure mode obtained by equation (8) for safety.

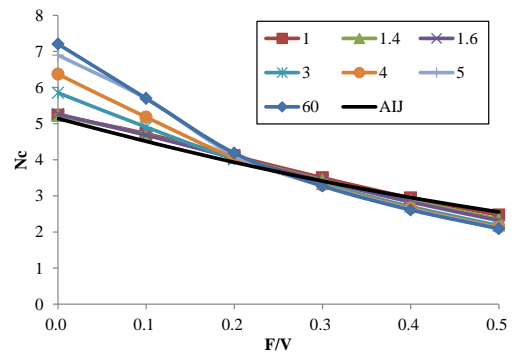


Fig. 6 Relationship between N_c and B/H (Analysis).

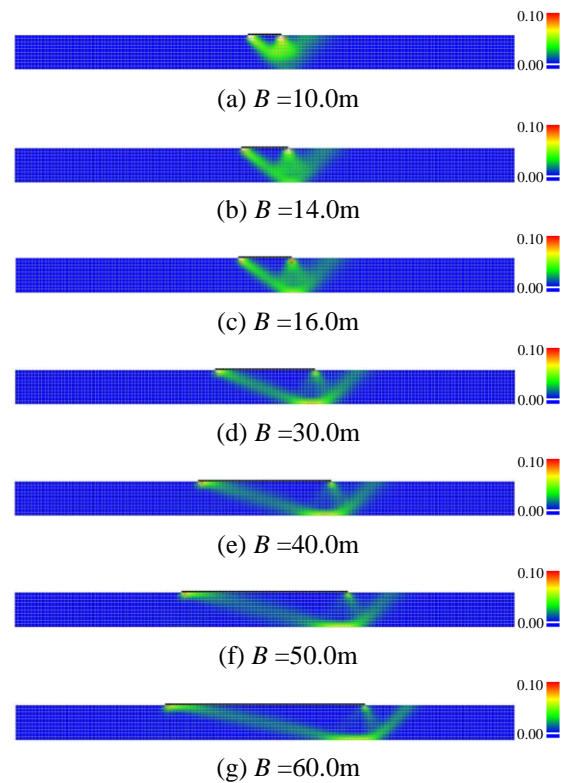
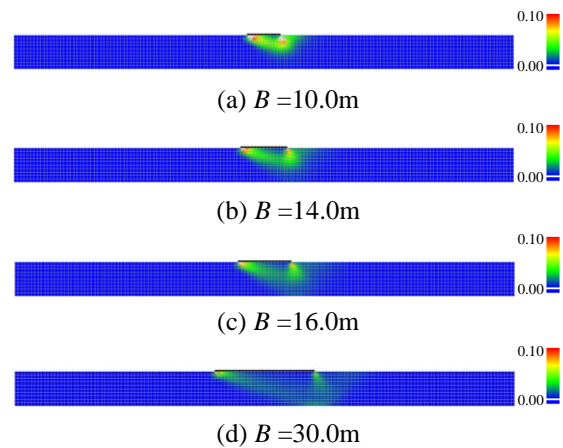


Fig. 7 Shear strain contour at $F/V=0.1$



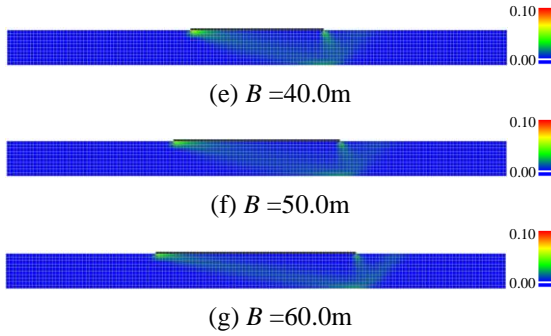


Fig. 8 Shear strain contour at $F/V=0.3$

4. SIMULATION OF CLAYEY SQUEEZE BREAKDOWN WITH INITIAL LOAD

4.1 Numerical conditions

In order to consider the load during an earthquake, the initial vertical load V_0 , horizontal load HT_0 , and moment M_0 were introduced as shown in figure 9. Both in-phase and anti-phase moments against the earthquake direction were considered. The ultimate vertical bearing capacity was calculated using rigid-plastic FEM under the initial load conditions listed in table 2. The unit weight of the building (3.3 stories, 10 kN/m^2 per floor) was assumed as $\gamma = 3 \text{ kN/m}^3$. Three cases with different spread widths (10 m, 30 m, 60 m) and five cases with different heights ($0.15B$, $0.25B$, $0.3B$, $0.5B$ and $1B$) were considered. The horizontal force and moment were assumed to be applied at the midpoint of building height. The inclined load was applied to the foundation as the distribution load divided into horizontal and vertical components. “Kh” refers to the horizontal seismic intensity.

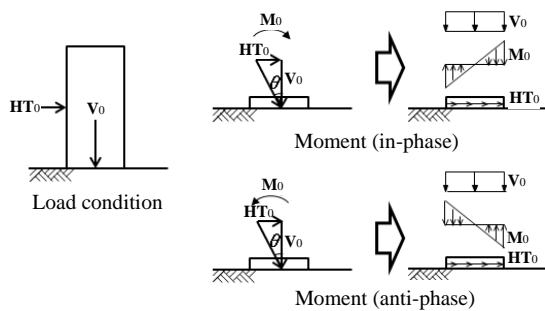


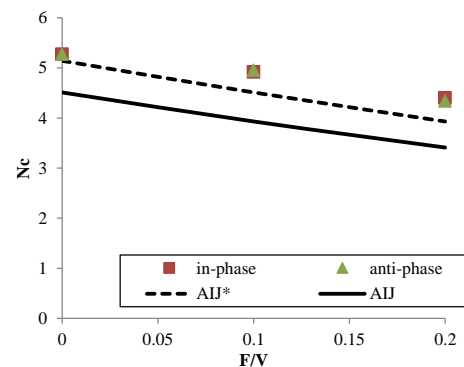
Figure 9 Initial load conditions for rigid-plastic FEM

Table 2 Analysis conditions

Foundation wide B (m)	10	30	60
Height H (m)	$1B$	$0.3B, 0.5B$	$0.15B, 0.25B$
Horizontal seismic intensity Kh	0.1, 0.2		
Moment direction	in-phase, anti-phase		

4.2 Numerical results

Figure 10 shows the results of the simulation. The AIJ and AIJ* results were calculated by equation (8) with considering initial inclined load (considering i_γ) and without considering initial inclined load (no considering i_γ). As with the inclination load consideration, the value of N_c decreased as F/V increased. The values obtained by numerical analysis were larger than those by AIJ. Equation 9 is a formula proposed in the case of increasing inclined load. In this analysis, there is an inclined load at the beginning and only the vertical load increases. There is a possibility that this analysis is overvalued. Compared with AIJ*, it corresponds well before the squeezing breakdown occurs, but when the squeezing breakdown occurs, it differs from the analysis result. Figure 11 shows the contours of the shear strain at failure at $B=10 \text{ m}$, $Kh=0.2$, $HT=1B$ and $B=60 \text{ m}$, $Kh=0.2$, $HT=0.15B$. For the first condition, each N_c was almost the same. Similar to the shear strain distribution, there are differences in the occurrence of shear faces on the left and right, but general failure mode occurs. In contrast, for the second condition, the value of anti-phase is larger than that for in phase. It is considered that the anti-phase mode is closer to the squeezing breakdown along only the vertical direction. In fact, when assuming a large earthquake, the assumed horizontal force and moment do not change, and the margin of the vertical bearing force is important. Because the value obtained by the analysis is larger than the value of AIJ including the examination of the previous inclined load, it can be said that the design specification of the AIJ entails lesser risk.



$B=10 \text{ m}$, $HT=1B$

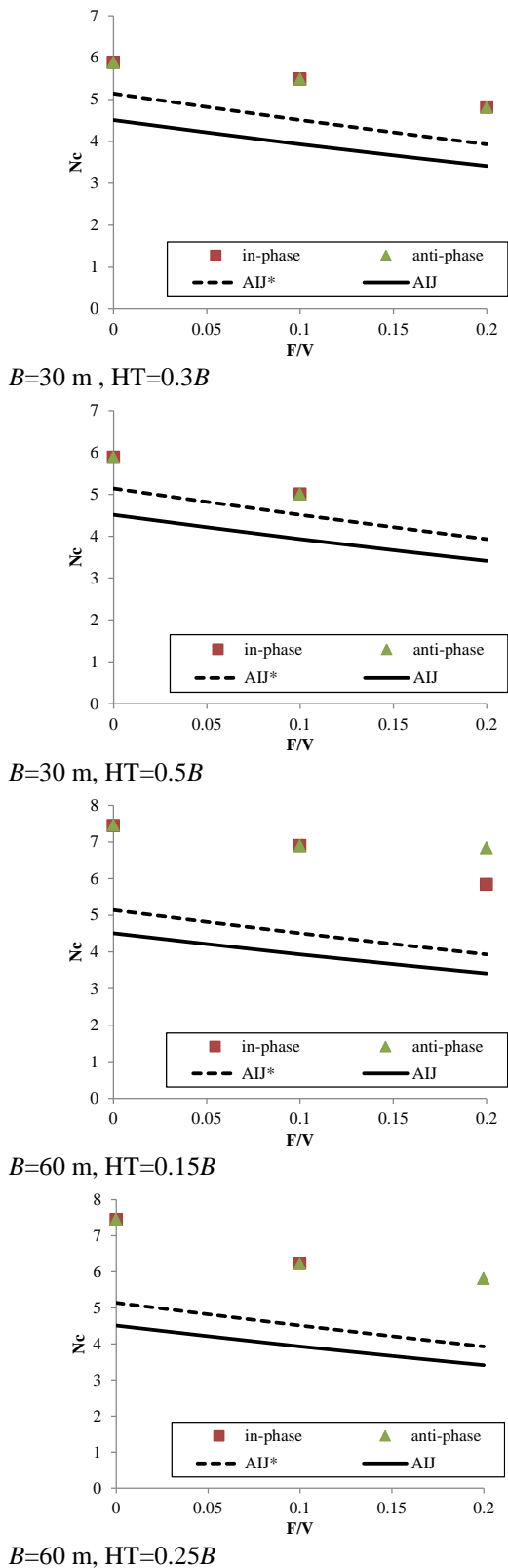


Figure 10 Relationship between N_c and F/V for in and anti-phase

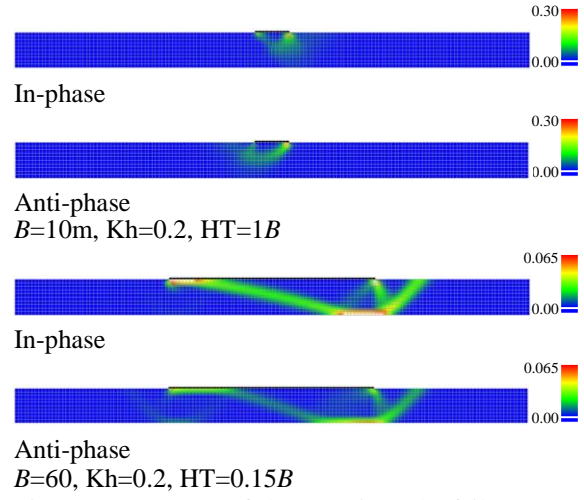


Figure 11 Contours of shear strain at the failure

5. CONCLUSION

The vertical failure mode changes from the general failure mode to squeezing breakdown with increasing B/H . At $B/H=3$, the cross-shaped failure mode occurred at the ground under foundation. Shearing blocks occurred at both ends of the foundation. For $B/H>4$, the cross-shaped failure mode cannot be seen and shear failure occurred from both sides of the foundation.

In the failure mode with inclined load, at small F/V , the failure mode differed depending on the B/H . For $F/V > 0.2$, the failure mode remained the same regardless of B/H . From the results of numerical analysis, it is considered that it is necessary to consider the corrective inclined coefficient for the general failure mode.

In the vertical failure mode with initial load, considering an earthquake, the N_c values were larger than those obtained by the AIJ equation. This further implies that it is necessary to consider the corrective inclined coefficient for the general failure mode.

6. REFERENCES

- [1] Terzaghi, K. and Peck, R.B. : Soil Mechanics in Engineering Practice, John Wiley & Sons, pp. 472-569. 1967.
- [2] Tamura, T., Kobayashi, S., and Sumi, T. : "Limit analysis of soil structure by rigid plastic finite element method", Soils and Foundations, Vol.24, No.1, pp.34-42.1984.
- [3] Asaoka, A. and Ohtsuka, S. : "The analysis of failure of a normally consolidated clay foundation under embankment loading", Soils

- and Foundations, Vol.26, No.2, pp.47-59, 1986
- [4] Yamaguchi, H. : Theory and applications of bearing capacity and deformation of shallow foundation, Soil Japanese Society of Soil Mechanics and Foundation Engineering , No.2, pp.85-91, 1982. (In Japanese)
- [5] Architectural Institute of Japan, AIJ (1988,2001), Recommendations for design of building foundation , pp.105-111, 2001. (In Japanese)
- [6] Kaneda, K., Tanikawa, T., Hamada, J., Ohtsuka, S., and Aoki, M.: “Analysis of ultimate bearing capacity of footing of two layered clayey soil system by rigid plastic finite element method”, AIJ Journal of technology and design, Vol.19, No.43, pp 881-885. (In Japanese)
- [7] Meyerhof, G.G. and Chaplin, T.K.: “The compression and bearing capacity of cohesive layers”, British Journal of Applied Physics, Vol.4, No.1. 1953.
- [8] Hoshina, T., Ohtsuka, S. and Isobe, K., Ultimate bearing capacity of ground by Rigid plastic finite element method taking account of stress dependent non-linear strength property, Journal of Applied Mechanics, 6, pp.191-200, 2011.
- [9] Nguyen, Du L., Ohtsuka, S., Hoshina, T. and Isobe, K., Discussion on size effect of footing in ultimate bearing capacity of sandy soil using rigid plastic finite element method, Soil and Foundations, vol.56, no.1, pp.93-103,2016.

Copyright © Int. J. of GEOMATE. All rights reserved, including the making of copies unless permission is obtained from the copyright proprietors.
